

CHAPTER IV

EXPERIMENTAL THEORY AND PROCEDURE

As stated in Chapter I, measurement of the infinite dilution diffusion coefficient D_{12} was the primary goal of this work. In addition, the solvent density and viscosity were also measured. In the first three sections of this chapter the theories for measuring these three physical properties are given. It should be emphasized that the experiment for measuring density is a novel procedure developed during the course of this work. In sections 4.4 and 4.5 the apparatus is described, and in sections 4.6 to 4.8 the calibration results for diffusivity, density, and viscosity measurements are presented. Section 4.9 gives the purity and composition of the liquids and gases used in the experiments.

4.1 Taylor Dispersion Theory for Diffusivity Measurement

In 1952, Sir Geoffrey Taylor was asked by a veterinarian to explain how the mean velocity of blood in the arteries of animals could be deduced from tracer studies (Taylor, 1954). Sir Taylor answered the question in his classic paper which explains a method to measure not only the mean velocity, but the diffusion coefficient of the tracer as well (Taylor, 1953). The method has become known as Taylor dispersion and has found widespread applications.

The idealized Taylor dispersion experiment can be described as follows. A narrow pulse of solute is quickly injected into a long uniform tube, in which a solvent is flowing in slow laminar flow. As the pulse is carried through the tube, it spreads due to the combined effects of laminar flow and molecular diffusion, although the peak center or maximum continues to flow at the mean velocity of the laminar profile. Eventually, the peak elutes from the end of the long tube, at

which point the radially averaged concentration profile is measured as a function of time. From this recorded concentration vs. time data, the diffusion coefficient can be determined using the mathematics derived by Taylor.

The differential equation describing the solute concentration is given below in standard cylindrical coordinates.

$$D_{12} \left(\frac{\partial^2 C}{\partial r^2} + \frac{1}{r} \frac{\partial C}{\partial r} + \frac{\partial^2 C}{\partial z^2} \right) = \frac{\partial C}{\partial t} + 2\bar{u} \left(1 - \frac{r^2}{a^2} \right) \frac{\partial C}{\partial z} \quad (4.1)$$

In this equation, C is the concentration, which is a function of radial position r , and the axial position z . D_{12} is the mutual diffusion coefficient, a is the tube radius, and \bar{u} is the mean solvent velocity.

Applying several simplifying assumptions which are easily satisfied in practice, Taylor showed that Equation 4.1 could be reduced to the following simplified equation;

$$K \frac{\partial^2 C_a}{\partial Z_1^2} = \frac{\partial C_a}{\partial t} \quad (4.2)$$

where

$$Z_1 = z - \bar{u}t \quad (4.3)$$

In Equation 4.2, C_a is the radially averaged concentration, and K is the effective Taylor dispersion coefficient. Z_1 is the axial coordinate which moves with the mean solvent velocity \bar{u} . Aris (1956) used the method of moments to show that the definition for K given in Taylor's original work was not complete. Using straightforward calculus and algebra, Hunt (1976) verified that Aris's definition for K was indeed correct and is given by:

$$K = D_{12} + \frac{\bar{u}^2 a^2}{48 D_{12}} \quad (4.4)$$

Taylor had neglected to include the first term on the right hand side of Equation 4.4. Taylor's assumption is often reasonable since in practice the first term is usually orders of magnitude smaller than the second term.

Equation 4.2 can be solved analytically for the case of a concentrated spike injection of mass M at time zero. The radially averaged concentration at the end of the diffusion tube, distance L from the injection point is given by;

$$C = \frac{M}{\pi a^2 (4\pi Kt)^{1/2}} \cdot \exp\left(\frac{-(L - \bar{u}t)^2}{4Kt}\right) \quad (4.5)$$

Surprisingly, even though this solution appeared in Taylor's (1953) original paper, it has not been used in its entirety to analyze actual data from any previous Taylor dispersion experiment.

Direct application of Equation 4.5 to determine K and hence D_{12} requires non-linear parameter estimation. Since much of the early Taylor dispersion work was completed prior to the advent of computers, non-linear techniques were considered impractical. Two techniques have emerged as the most popular methods for Taylor dispersion data analysis. These techniques will be referred to as the "graphical method" and the "moment method."

A highly approximate graphical data analysis method has been used by several researchers including Sun and Chen (1985) to analyze Taylor dispersion data. The graphical method is based on an approximate solution to Equation 4.2 originally derived by Giddings and Seager (1962) and Cloeta (1976). The graphical method is given by the following equations, where $W_{1/2}$ is the dispersion peak width at half height, and t_{max} is the time corresponding to the peak maximum.

$$D_{12} = \frac{\bar{u}}{4} \left[H - \left(H^2 - \frac{a^2}{3} \right)^{1/2} \right] \quad (4.6)$$

where

$$H = L(W_{1/2})^2 / (5.54t_{max}) \quad (4.7)$$

The method is termed the "graphical method" since the peak maximum and half width are usually measured from a recording chart with a ruler. The method has two obvious drawbacks; (1) the mathematics of the method are approximate, and (2) the method is subject to human measurement errors.

The moment method solution to Equation 4.2 was given by Aris (1956) and later explained more clearly by Alizadeh et al. (1980). In its simplest form, the solution is;

$$D_{12} = \frac{a^2 \bar{t}}{24\sigma^2} \quad (4.8)$$

where:

$$S = \int_0^\infty C_a(t) dt \quad (4.9)$$

$$\bar{t} = \frac{1}{S} \int_0^\infty t C_a(t) dt \quad (4.10)$$

$$\sigma^2 = \frac{1}{S} \int_0^\infty (t - \bar{t})^2 C_a(t) dt \quad (4.11)$$

Equations 4.9 through 4.11 are the zeroth, first, and second temporal moments of the dispersion peak. In practice, the moments are usually calculated from the raw peak data by finite summation using the trapezoidal rule. Close examination of Equation 4.11 reveals that the second temporal moment, or variance, is heavily weighted at the peak ends by the difference term. This weighting, where the measurement uncertainty is greatest, can result in large errors in the resulting diffusion coefficients calculated using Equation 4.8. The disadvantages of the moment method are discussed in detail by Radeke (1981). We originally analyzed most of our diffusivity

data using the moment method, but encountered difficulties in determining peak starting and ending points.

In order to avoid the inherent errors associated with the moment and graphical methods, we developed a new analysis method based on the analytical solution to the Taylor dispersion problem. The new method was used to reanalyze all of our diffusion data. Before describing the method, it is necessary to explain how concentration is measured in a practical apparatus. In most Taylor dispersion apparatuses, including our own, concentration is not measured directly. Instead, a detector at the end of the diffusion tube outputs a voltage which is proportional to the solute concentration. Theoretically, the detector output voltage should remain steady when a peak is not eluting, but in practice the output often drifts linearly with time.

We developed a mathematical model based on Equation 4.5, Taylor's original analytical solution which models the detector output voltage, V , as follows:

$$V = \frac{B_1}{t^{1/2}} \cdot \exp \left[\frac{-(L - B_4 t)^2}{B_2 t} \right] + B_3 + B_5 t \quad (4.12)$$

The B terms are free parameters which must be fit to the data. B_3 and B_5 account for baseline offset and drift. B_4 is the average solvent velocity in the diffusion tube. B_2 is simply a factor of four times greater than K , the effective Taylor dispersion coefficient. Once K is known, the diffusion coefficient can easily be determined by solving Equation 4.4 for D_{12} using the quadratic formula.

Voltage and time data are recorded concurrently by computer at regular intervals. Using this data, the best fit parameters for Equation 4.12 are determined using non-linear least squares analysis. The Newton-Raphson iterative technique is

used to determine the set of B 's which minimize the following function;

$$F = \sum_{i=1}^n [V_{meas.}(i) - V_{Eq.4.12}(i)]^2 \quad (4.13)$$

The Newton-Raphson method requires both the first and second derivatives of Equation 4.13 with respect to each B . We determined analytical expressions for these derivatives in order to negate the possibility of roundoff errors and to assure quick convergence.

Reasonable initial guesses for the model parameters are crucial for convergence to be achieved. We generate all of the initial guesses internally within a computer program containing the model. Highly accurate guesses for B_1 and B_2 are determined by employing a search routine to find the peak maximum and then applying simple algebraic relationships which exist between the model and the analytical solution. Accurate estimates for baseline slope B_3 , and baseline drift B_5 , are easily determined from the starting and ending points of the peak. The difficulty lies in estimating B_2 , which is analogous to estimating the Taylor dispersion coefficient K apriori. By using a computerized version of the graphical method, presented earlier in this section, we are able to generate initial guesses for B_2 which lead to rapid convergence. Figure 4.1 illustrates the excellent agreement between measured voltage and voltage predicted by Equation 4.12 for an actual peak measured during this study. For this peak, voltage was measured every 5 seconds, but is plotted only every 30 seconds in Figure 4.1.

The entire method for Taylor dispersion data analysis is incorporated into one user-friendly computer package. The only required user input is the time of injection and the approximate interval in time where the peak was recorded. The new analysis method allows for quick and accurate determinations of the diffusion

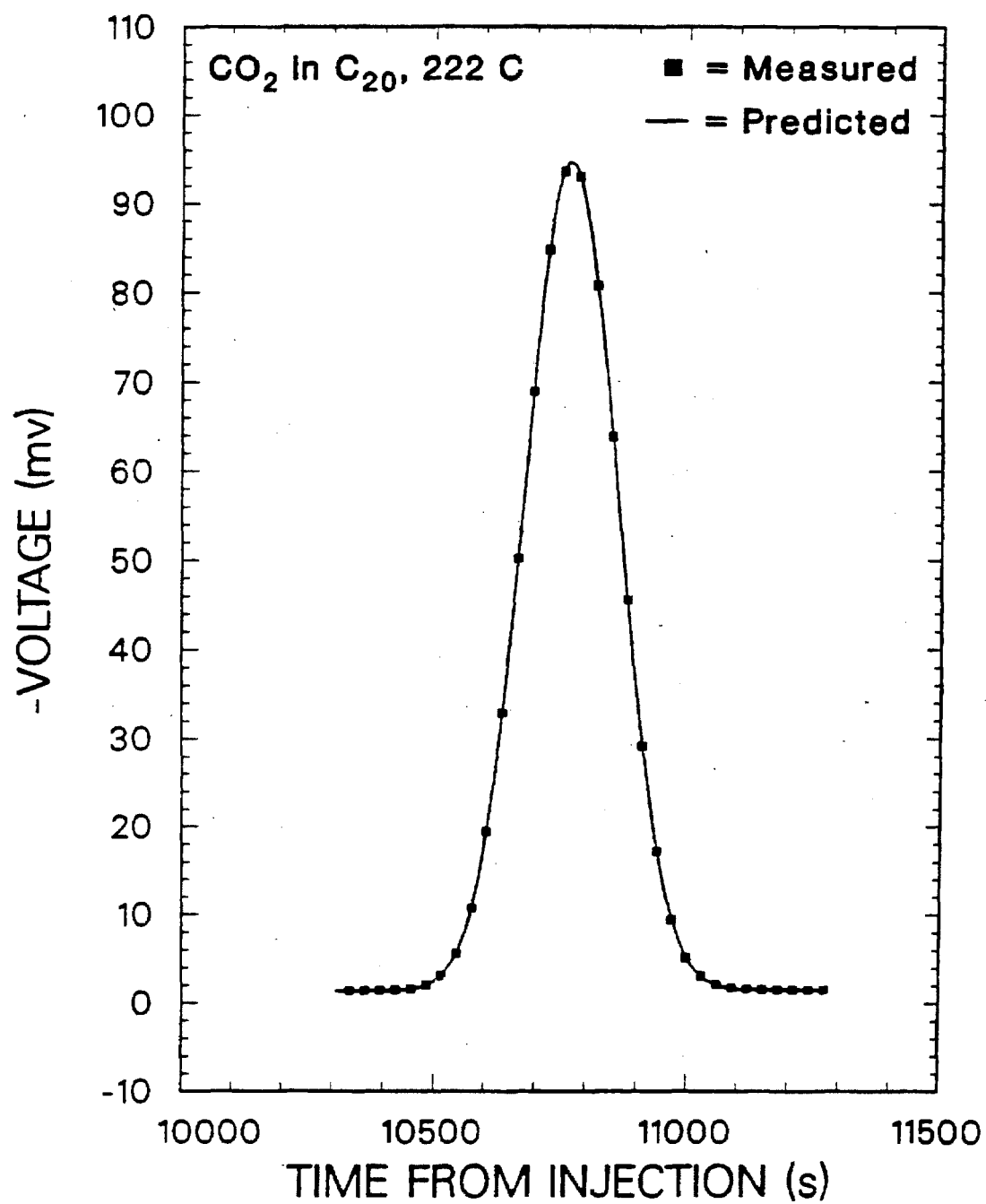


Figure 4.1. Actual comparison of raw peak data to the best fit prediction of Equation 4.12.

coefficient without the inherent uncertainties of the approximate methods currently in use.

4.2 Density Measurement from Taylor Dispersion Results

Density is an important parameter occurring in most correlations for the diffusion coefficient. Often density does not appear in these correlations directly, but is disguised as molar volume, the quotient of molecular weight and density.

We have recently reported an original technique, developed during this project, which allows solvent density to be accurately measured using a Taylor dispersion apparatus (Matthews and Akgerman, 1987c). The technique is based on the fact that solvent density is related to the Taylor dispersion peak retention time and solvent mass flow rate. First, a calibration experiment is performed with a solvent of known density, such as water. Then using the mass flow rate and peak retention time from this calibration experiment, the density of any other solvent at any conditions may be determined from:

$$\rho_2 = \rho_1 \frac{\dot{m}^{(2)} \bar{t}^{(2)} V_t^{(1)}}{\dot{m}^{(1)} \bar{t}^{(1)} V_{t(2)}} \quad (4.14)$$

where the retention time is given by:

$$\bar{t} = L/\bar{u} \quad (4.15)$$

The ratio of tube volume at the calibration temperature to volume at the experimental temperature is easily calculated using the thermal expansion coefficient for the tube material. The actual tube volume does not need to be calculated.

We have used the Taylor dispersion apparatus to measure solvent density at each temperature where diffusion coefficients were measured. The data are needed for correlating diffusion, and are especially important since few measurements of liquid density have been made for many of the chosen solvents.

4.3 Viscosity Measurement

The viscosity of Newtonian solvents may be measured by the well-known capillary viscometer technique, which is based on the Hagen-Poiseuille equation:

$$\eta = \frac{\pi \Delta P R^4}{8 Q L} \quad (4.16)$$

where Q is the volumetric flow rate of the solvent, η is its viscosity, and ΔP is the resulting pressure drop across the capillary. This technique is the natural choice to be used in conjunction with the Taylor dispersion method since both require that the solvent be moving in laminar flow. The pressure drop measurement may be influenced by entrance effects (Bird *et al.*, 1960), but under the conditions of the present experiments these were found to be negligible.

4.4 Description of Apparatus

This section describes our original Taylor dispersion apparatus which was constructed during the first phase of the project. The original apparatus was used to collect data in the solvents n-heptane, n-dodecane, and n-hexadecane, which are all liquids at room temperature. In the following section, we explain the modifications which were performed to this original apparatus to allow operation with the solvents n-eicosane, n-octacosane, and Fischer-Tropsch wax, which are all solids at room temperature. Most of these modifications were external, and did not significantly affect the basic operation and dimensions of the apparatus as described in this section.

Our original Taylor dispersion apparatus has been described in detail by Matthews and Akgerman (1987a) and is shown in Figure 4.2. The apparatus was constructed in accordance with the design criteria given by Alizadeh *et al.*

(1980). Solvent flow rates were chosen to meet the criteria given by Hunt (1976) and Alizadeh et al. (1980). These criteria ensure that the approximations inherent to the mathematics of Taylor dispersion are satisfied in the experiment and that secondary flow effects due to coiling are negligible.

In general the apparatus operates as follows. Solvent is pumped from a tank into the heated enclosure where the capillary viscometer is located. After leaving the viscometer, solvent flows out of the heated enclosure for a short time to the reference side of a refractive index detector, where a baseline signal is established. Solvent then flows back into the heated enclosure where the sample is injected and dispersion occurs. The dispersed sample pulse then flows out of the enclosure to the sample side of the detector, where a signal is generated due to the difference in refractive indices between the sample and reference sides. The signal is recorded as a function of time by a computer so that the response curve may be analyzed following the experiments. Usually a series of sample pulses are injected so that several response curves may be obtained at close spacings, thus allowing for rapid accumulation of diffusivity data.

The first operational step was to fill the feed tank with the desired solvent. After each filling of the solvent tank, the solvents were vigorously sparged with helium to remove air and absorbed moisture, and then a slow sparge was continued. The solvent pump was an LDC/Milton Roy Constametric III with the slow speed option. Flow rates were typically 0.1 to $0.3 \times 10^{-6} \text{ m}^3/\text{min}$ (0.1 to 0.3 ml/min). This allowed us to operate at Reynolds numbers less than 15 in the diffusion coil. Prior to the diffusion coil, the solvent was pumped through 3 m of 0.00025 m i.d. capillary tubing to provide a resistance to flow, which helped damp out pulses from the solvent pump. When n-heptane was used as the solvent, it was found helpful to

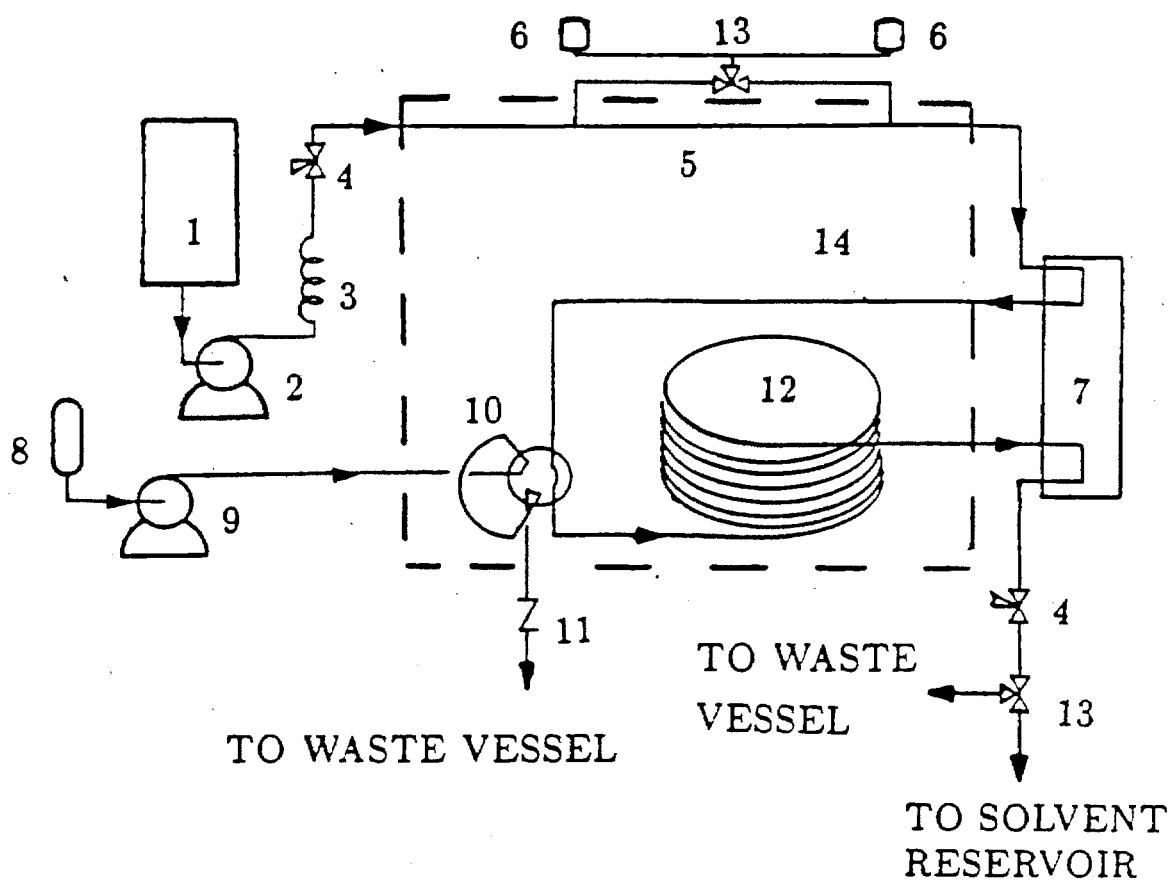


Figure 4.2. Schematic diagram of Taylor Dispersion Apparatus. 1. Solvent reservoir. 2. Solvent pump. 3. Capillary tube flow restrictor. 4. Backpressure regulators. 5. Capillary tube viscometer. 6. Pressure transducers. 7. Refractive index detector. 8. Sample solution. 9. Sample injection pump. 10. 6-port sample injection valve. 11. Needle valve. 12. Coiled dispersion tube. 13. 3-way valves. 14. Heated enclosure.

use a Grove backpressure regulator set at 6.9 MPa to provide additional damping of the pump. The pressure of the experiment was controlled by a second Grove regulator located downstream of the detector.

Solvent was pumped at ambient conditions into the heated enclosure which contained the capillary viscometer, the diffusion tube, and the sample injection valve. The solvent passed through a 3 m length of preheat tubing before entering the capillary tube viscometer. Two calibrated strain gauge pressure transducers (Teledyne Taber model 2201) were installed on a valve manifold so that upstream and downstream pressure on the viscometer tube could be measured with each transducer. This gave redundant values of ΔP which could be compared for consistency.

After the viscosity measurement, solvent flowed out of the heated enclosure to the reference cell of the detector, an LDC/Milton Roy Refractomonitor III differential refractive index detector. Temperature in the detector cell was maintained at 313 K with a Fisher Model 80 circulating water bath. The detector cell was modified for the high pressures of the experiments by installing a Kalrez^R gasket under the refractive prism and by removing the metal shim under the prism.

From the reference side of the detector, the solvent returned to the heated enclosure where the sample was injected. The injection valve was a Valco Instruments model A6C6WT which could operate at up to 573 K and 45 MPa. The solute solution was either 4 or 8 mole percent of solute dissolved in the solvent, and was prepared external to the heated enclosure and pumped into the sample loop. Pressure on the sample loop was maintained with a fine metering valve. By use of the high temperature injection valve, the sample was injected at the same temperature and pressure as the diffusion tube. This eliminated any additional variance caused

by the sample pulse heating or by the sample being compressed as it entered the diffusion tube. An additional feature of the injection valve is that it was driven by a pneumatic actuator and switched by a Valco Digital Valve Interface. This caused switching of the valve in about 10 milliseconds, effectively eliminating any interruption of solvent flow during sample injection (Harvey and Stearns, 1984).

Following injection, the pulse flowed into the diffusion tube, which was a 43.55 m stainless steel tube coiled on a supporting cylinder of aluminum. Retention time in the diffusion tube was typically on the order of 3 hours. The dispersed solute peak then moved to the sample side of the refractive index detector where a signal was produced. After leaving the detector, the solvent flowed through the second backpressure regulator. A three-way valve on the outlet allowed diversion of solvent to an external vessel during experiments. The mass flow rate for density measurements was obtained by weighing this vessel and calculating the mass collected during a known time period. At other times, the solvent was recirculated to the solvent tank, thus eliminating any delays in the start-up of experiments. Except when troubleshooting or changing solvents, the solvent was left circulating continuously, even when the apparatus was unattended.

The heated enclosure was constructed from aluminum pipe. The diffusion tube was coiled on a ring which fit snugly inside the pipe. The ends of the enclosure were covered with aluminum plate, and the void space inside the enclosure were filled with aluminum shot so that the system was thermally massive and stable, with good internal heat conduction. The upper temperature limit of the enclosure containing the diffusion coil is approximately 573 K. All physical dimensions of the apparatus are given in Table 4.1.

Because the Taylor dispersion experiment lends itself to automation, micro-

Table 4.1 Physical Specifications of Taylor Dispersion Apparatus and Capillary Viscometer

Description	Value \pm Uncertainty
Length of Dispersion Tube (m)	43.55 ± 0.05
Radius of Diffusion Tube (m)	0.000523 ± 0.000005
Length of Connecting Tube (m)	0.52 ± 0.01
Radius of Connecting Tube (m)	0.000127 ± 0.000005
Radius of Diffusion Tube Coil (m)	0.157 ± 0.008
Height of Cylindrical Heated Enclosure (m)	0.406 ± 0.006
Volume of Detector Cell (10^9 m^3)	9
Capillary Viscometer Length (m)	1.034 ± 0.0021
Viscometer R^4 (10^8 cm^4)	3.971 ± 0.035

computer aided data acquisition and control were used. A schematic of the control system is given in Figure 4.3. Two Commodore B-128 personal computers were used as controllers. Due to the limitations of the Commodore 128's, one computer was dedicated to on-line monitoring of the detector signal. This was done by reading the detector output with a Keithly 197 digital voltmeter. Data were transmitted to the computer via an IEEE-488 bus and recorded on disk. Following the experiments, this data was uploaded to our Chemical Engineering Department's computer, a Hewlett-Packard 9000, where it was analyzed to determine values for D_{12} .

The second computer was used for monitoring pressure and temperature, and also for controlling the temperature in the enclosure. There were six calibrated thermistors located at various positions within the enclosure. These six signals, with the two pressure transducer signals, were networked in a Keithly Model 705 programmable multiplexer. The computer controlled the signal scanning sequence, and signals were read on a Solartron Model 7150 digital multimeter. Data were transmitted to the computer via an IEEE-488 bus, where the temperature and pressure were calculated using calibration equations. A digital PI temperature

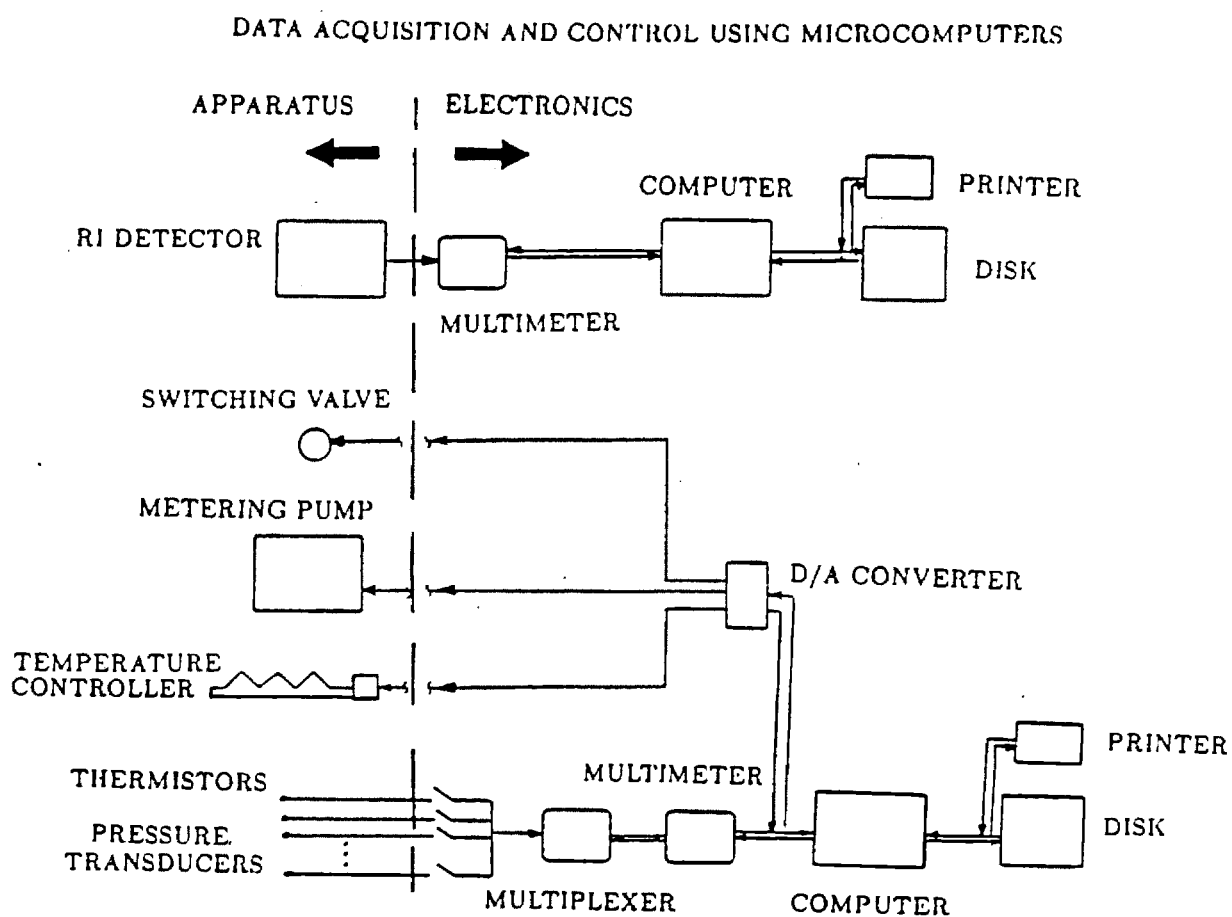


Figure 4.3. Schematic of data acquisition and control system.

controller algorithm was also programmed, and the heater firing rate controlled via a Connecticut Microcomputer D/A output converter. The temperature could be controlled to better than ± 0.5 K during the course of an experiment.

The temperature of the experiment was obtained by averaging the readings from the six thermistors which were placed at various locations around the periphery of the diffusion tube. The thermistors were individually calibrated against a standard platinum resistance thermometer. The calibrations were performed twice to check for reproducibility. The first calibration covered 15 temperatures between 303 and 503 K, and the second covered 27 temperatures between 298 and 570 K. It was found that the predicted temperatures obtained from these two calibrations agreed to within 1 K of each other. Within the apparatus there were small temperature gradients which usually did not exceed 0.5 K. We reduce the effects of gradients and systematic error by averaging, and consequently feel that the uncertainty in the reported temperatures is no more than 1 K.

The pressure transducers were also calibrated twice, once against a DH Instruments dead weight pressure gauge and once against a Ruska dead weight gauge. In both cases the transducer responses were linear with pressure, and the differences in predicted pressure were in error by less than 1.4 kPa (0.2 psi) over the range of pressures between 1400 and 3500 kPa (200 to 500 psia). Over the course of time there was a drift in the zero of the transducers increasing the uncertainty to about 7 kPa (1 psi).

4.5 Modifications to Original Apparatus

The original apparatus was extensively modified before data was collected using the solvents *n*-eicosane, *n*-octacosane, and Union Carbide FT wax, which are all

waxy solids at room temperature. All wetted parts of the apparatus needed to be maintained safely above the melting point of the circulating solvent. The limiting solvent was Fischer-Tropsch wax which melts at approximately 100°C. In order to safely meet this criteria, all modifications were designed to withstand at least 130°C.

The following modifications were necessary;

1. All external lines, valves, and backpressure regulators were heat traced with electrical heating tape. Most external lines were physically rerouted for safety and convenience. Valves were remounted on a panel. It was also necessary to change some valve packings and all seals to withstand the elevated temperatures.
2. The chromatographic pump (LDC/Milton Roy Constametric) piston seals were replaced with high temperature seals obtained from the manufacturer. The hydraulic section of the pump was heat traced with electrical heating tapes. Provisions were made for separating the heated hydraulic section of the pump from the pump electronics, but these provisions did not prove to be necessary. Through careful control and maintenance, we were able to successfully operate the pump at 130°C, which was far beyond the maximum operating temperature of 70°C suggested by the manufacturer.
3. We have separated the optics from the electronics of the detector. The optical portion of the refractive index detector (LDC/Milton Roy Refractomonitor III) which contains the wetted cell was removed from its housing and mounted in a custom made enclosure. This prevented damage to the sensitive electronics of the detector due to heat and/or accidental liquid leakage. The cell and entrance tubing was heated by circulating hot ethylene glycol through a jacket surrounding the cell assembly. The gasket separating the sample and reference sides of the cell was replaced with a custom high temperature gasket. These modifications produced the first differential refractive index meter capable of operating above 70°C. In fact, for the Fischer-Tropsch experiments, we amazed the manufacturer by operating the detector cell continuously at 145°C for a period of approximately five days. We found that it was necessary to operate the detector at this temperature with the FT wax in order to prevent a film from forming on the surface of the detector's prism.
4. A glass solvent feed tank with heating mantle and temperature controller was installed. A custom top with appropriate fittings was constructed.
5. All heated lines, valves, surfaces, etc. were well insulated.

6. The sample delivery system was modified as necessary so that it can be heated.

In addition to the temperature limitations of the detector, the detector is also limited by solids content and clarity. Any suspended solids interfere with the light beams of the detector and distort the signal. The manufacturer recommends using only prefiltered solvents (to $< 2\mu\text{m}$). Solids also have a tendency to collect in the cell of the refractive index detector. Although solvent color can be tolerated by the detector, the color must be uniform, and the liquid may not be turbid. We could not operate with the Mobil FT wax originally supplied by the DOE for several reasons; (1) the melting point was too high to be tolerated by either the detector or the pump; (2) the sample was turbid; and (3) the solids content was intolerable. Although the solids may have been filtered, the problems of temperature limitations and solvent turbidity could not be overcome. The sample of Union Carbide FT wax which was used did not present any of these problems. A detailed description of the Union Carbide wax is included in Section 4.9.

Our experiments using gaseous solutes were originally conducted by injecting samples of solvent which had been saturated under pressure with the gaseous solute. During the course of these experiments, several accidental injections of pure gas occurred. Although the resulting dispersion peaks were much larger than the corresponding peaks for the saturated liquid injections, the calculated diffusion coefficients for the two types of injections agreed within experimental error. We investigated this phenomenon further and were able to develop a reliable technique for collecting gas-liquid diffusion data by injecting minute quantities of pure gas under pressure. This technique eliminated the need for an external saturator and greatly simplified the experiment.

4.6 Calibration for Diffusivity Measurements

Before extensive data gathering could proceed, three calibration experiments were made. The first of these was to insure that the signal given by the detector was a linear function of the concentration of the solute. A lack of linear behavior would render invalid the use of either of the mathematical analysis techniques which were discussed earlier in this Chapter. To determine the detector linearity, the Taylor dispersion experiment was performed five times, using five different solute concentrations. The sum function was calculated (equation 4.9) and plotted versus the sample mole fraction in Figure 4.4. Within experimental error, the response was a straight line with intercept zero, indicating that the detector response was indeed linear.

The second calibration experiment concerned the effect of coiling the diffusion tube. It is well known that the parabolic laminar velocity profile can be disrupted by the effect of secondary flows caused by flow of fluid in a curved path. Alizadeh *et al.* (1980) recommend that the following criteria be observed to keep the effect of secondary flows less than 0.5%:

$$De^2 Sc < 20 \quad (4.17)$$

where De is the Dean number $= Re/\sqrt{R/R_c}$ and Sc is the Schmidt number $= \eta/\rho D_{12}$. In these equations R_c is the radius of the tube coil, R is the radius of the diffusion tube, and Re is the Reynolds number $= 2Ru_a\rho/\eta$. Atwood and Goldstein (1984) give the following equation for estimating the effect of secondary flows on the true diffusion coefficient D_{12} :

$$D_{obs}/D_{12} = \frac{1}{1 - 0.1034(Q/Q_{trans})^4} \quad (4.18)$$

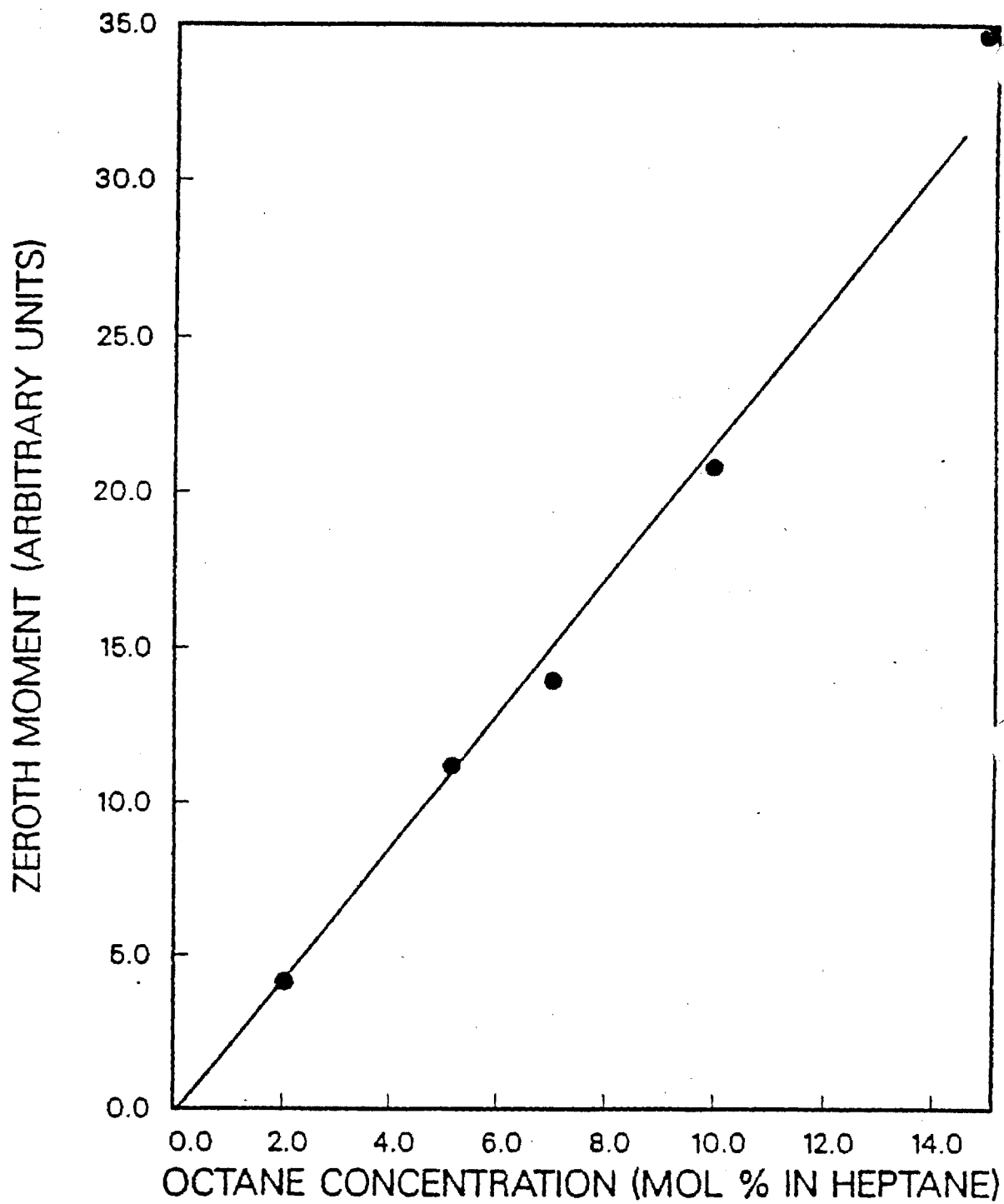


Figure 4.4. Linearity of detector response. Solute: n-octane. Solvent: n-heptane.

where Q is the flow rate of the experiment and Q_{trans} is the flow rate at which secondary flows begin to occur. From Atwood and Goldstein (1984):

$$Q_{trans} = (518RR_c D_{12} \eta / \rho)^{1/2} \quad (4.19)$$

The effect of increasing flow rate (or decreasing retention time) is shown in Figure 4.5 where the observed diffusion coefficient for n-octane in n-heptane at 298 K is plotted versus retention time. Obviously as retention time decreases the observed diffusivity increases well above the true value. The results of Figure 4.5 were used to guide the choice of flow rate for future experiments.

Because the magnitude of the diffusion coefficient and the viscosity vary greatly with temperature and with the particular solvent being studied, it is necessary to check the design criteria for each experiment. As part of the calculations for each experiment, the design criteria were evaluated and it was verified that we were operating within the required limits. For each measurement, we calculated $De^2 Sc$ and the ratio D_{obs}/D_{12} from equations (4.17) and (4.18) and found that the effect of secondary flows on our measurements was always less than 0.2%.

As a final confirmation of the proper design of the diffusivity apparatus, a comparison of some of our measured values with experiment is shown in Table 4.2. The agreement is within 3% for all values, which is remarkable considering the wide disparity of values for most liquid diffusion data which has been duplicated in the literature. Because the Taylor dispersion technique is simpler and less subject to error than the most earlier methods, we tend to trust our measurements more than the previously reported values.

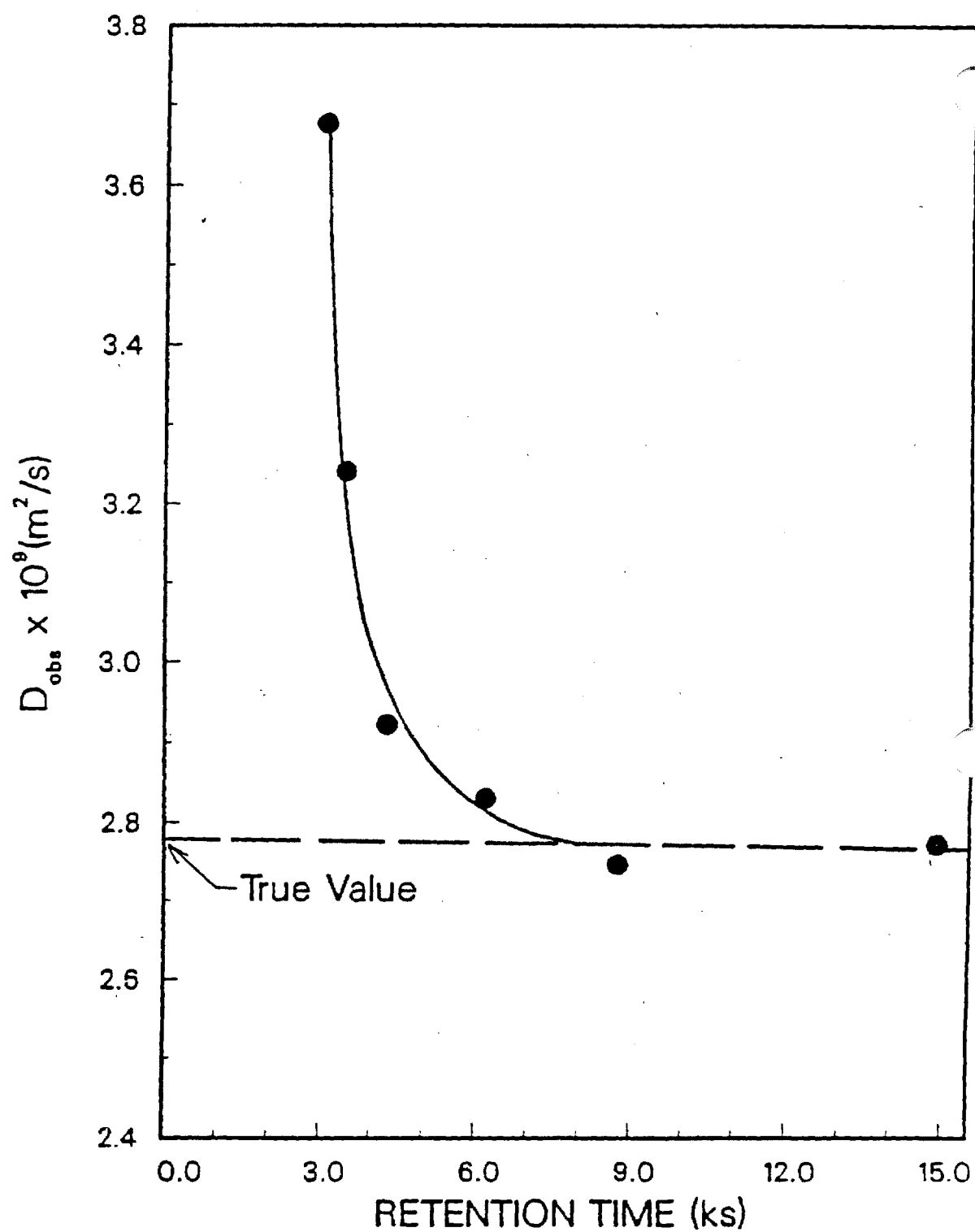


Figure 4.5. Secondary flow effects at high flow rates.

Table 4.2. Comparison of Diffusion Coefficients at Infinite Dilution
In the Solvent n-Heptane at 298 K and 0.1 MPa
($10^9 D_{12}, \text{m}^2/\text{sec}$)

Solute	This Work	Literature
octane	2.82	2.80 ¹
dodecane	2.21	2.15 ²
tetradecane	1.92	1.89 ²
hexadecane	1.83	1.78 ³

1. Alizadeh and Wakeham (1982). Technique: Taylor Dispersion.
2. Lo (1974). Technique: Diaphragm Cell.
3. Bidlack and Anderson (1964). Technique: Optical diffusimeter.

4.7 Calibration for Density Measurements

Distilled, deionized water was used as the calibration fluid since very accurate density data are available over a wide range of temperatures and pressures (Haar *et al.*, 1984). We performed two calibrations at 303.2 and 303.0 K to get a measure of reproducibility. The values of \bar{m} , \bar{t} , and ρ for the calibrations are given in Table 4.3. (The density values are from Haar *et al.*, 1984.) In the calibration experiments, a 2% by weight solution of methanol in water was used as the tracer solute.

To verify the proposed new procedure, the density of water was calculated from Taylor dispersion experiments performed at temperatures of 329, 354, and 392 K. Two experiments were done at each temperature, one using methanol as tracer and one using isopropanol. The purpose of using two tracers was to ensure that the nature of the tracer used had no effect on the measured density. At each temperature, the tube volume was corrected using the thermal expansion coefficient for austenitic (Type 316) stainless steels. The volume correction term for equation (4.14) is:

$$\frac{V_t^{(1)}}{V_{t(2)}} = \frac{(R^2 L)_1}{(R^2 L)_2} = (1 + \alpha \Delta T)^{-3} \quad (4.20)$$

where $\Delta T = T - 303 \text{ K}$. The value of α was obtained by a linear fit of the data given

Table 4.3. Calibration Data Using Water at 303 K as Reference Fluid.

Quantity	Calibration Number	
	1	2
$\dot{m}(10^{-3} \text{ kg/min})$	0.17762	0.17750
$\bar{t} \text{ (sec)}$	12,517	12,518
$T \text{ (K)}$	303.2	303.0
$P \text{ (kPa)}$	392	396
$\rho(10^{-3} \text{ kg/m}^3)$	0.995785	0.99579

Table 4.4. Measured and Literature Densities of Water Using Taylor Dispersion Data

T (K)	P (kPa)	Measured ρ (10^{-3} kg/m^3)	Literature ρ (10^{-3} kg/m^3)	Error ² (%)
330	396	0.98523	0.98512	+0.01
329	396	0.98534	0.98522	+0.01
354	396	0.97103	0.97125	-0.02
354	394	0.97117	0.97125	-0.008
392	394	0.94342	0.94397	-0.06
393	394	0.94344	0.94341	+0.003

1. Literature values from Haar *et al.* (1984).

2. Error = $100 \times (\text{Measured} - \text{Literature}) / \text{Literature}$

in Table 6-46 of the Chemical Engineer's Handbook (Perry and Chilton, 1973).

The resulting equation for alpha is given by the following equation;

$$10^6 \alpha \text{ (m/m} \cdot \text{K)} = 16.46 + 0.00424(T - 21\text{K}) \quad (4.21)$$

Table 4.4 gives the resulting calculated values of water density and the comparison with true values. The agreement is excellent, the average absolute deviation being 0.025 %. The slightly larger errors at 392 K are due to small thermal gradients within our apparatus which limit the accuracy of the temperature measurement. For water, an uncertainty in temperature of $\pm 0.5 \text{ K}$ at 393 K and 390 kPa corresponds to an uncertainty in density of about 0.05 %. We conclude that using the retention time \bar{t} from the Taylor dispersion experiment is an accurate

way of calculating the density of the solvent, and that correcting the tube volume for thermal expansion will give accurate results. A discussion of this new method is given by Matthews and Akgerman (1987c).

4.8. Calibration for Viscosity Measurements

A review of the capillary viscometer technique was given by Marvin (1971) in which the experimental error was thoroughly discussed. For this work, we desired an accuracy of $\pm 2\%$ or better, and to achieve this level the most critical factor is determining the value of R^4 to be used in the Hagen-Poiseuille equation (4.16). Direct determinations of the radius are not sufficiently accurate; the accepted way to determine R^4 is to calibrate the capillary tube with a fluid of known viscosity. The universal calibration fluid is water; accordingly, we calibrated the viscometer with distilled, deionized, degassed water at 294.8, 295.2, and 295.3 K. To account for thermal expansion, the viscosity of water was measured at 391.6 K, with the length and radius being corrected for thermal expansion as described previously. The results differed from literature values by less than 1%.

The viscosity data measured during this study were required to evaluate previous correlations for predicting diffusion coefficients. We originally thought that the viscosity data would be required to develop a new high temperature correlation, but we were able to develop a correlation which does not require viscosity data. This correlation is discussed in Chapter V.

4.9. Solute and Solvent Purity

Normal heptane, octane, hexadecane, eicosane, and octacosane were obtained from Alfa Chemicals. Normal dodecane was obtained from Phillips Petroleum. All

purities were stated as at least 99 mol%. All bottled gases were used as received.

The sample of Fischer-Tropsch wax used in this study was generously donated by Union Carbide via Dr. G. Sturm of the National Institute for Petroleum and Energy Research (NIPER) Center. The sample was originally sent to Dr. R.P. Anderson of NIPER on December 1, 1986. Fischer-Tropsch wax was sampled from a reactor using a cobalt catalyst. A similar sample of Union Carbide FT wax was analyzed by UOP (McArdle et al., 1986). For this whole wax sample, the carbon number distribution was found to range from C_{12} to C_{196} . The average carbon number was found to be 28. Only 0.45% of the carbons were branched, indicating a high percentage of n-paraffins.

A portion of the actual Fischer-Tropsch sample we obtained was analyzed by NIPER (Anderson, et al., 1987). Results for the whole wax sample are not yet available. However, an analysis of the heavy fraction containing only compounds with carbon numbers greater than C_{22} has been completed. This fraction was 80% alkanes and 7% olefins. The olefins were primarily mono-olefins.

From the information we have regarding the Fischer-Tropsch wax, it can be concluded that the sample contained at least 75% paraffins of which most were n-paraffins. The average carbon number was approximately 28. These general characterizations will prove useful when we discuss the diffusion coefficients measured in the Fischer-Tropsch wax.

The Union Carbide FT wax sample was a soft milky white solid, which could easily be stirred. Throughout the sample, clear liquid droplets could be observed. Upon heating, the sample began to melt at approximately 60°C , but was not a consistent uniform liquid until 110°C . Above 110°C , the liquid was clear, but had a yellowish tint. Upon cooling and freezing the yellow tint disappeared and the solid

returned to its original white color. We did not measure the boiling point of the wax, but UOP found the boiling point of a similar sample of Union Carbide wax to be 286°C.

We observed that when heated slowly, a clear phase formed below the predominant organic phase. This phase was analyzed by Karl Fischer titration and found to be at least 90% water. We carefully distilled the sample at 110°C under slight vacuum to remove the water. The distillate recovered represented 7% of the total liquid volume of the wax, and was primarily an aqueous phase. It was absolutely necessary to remove this water phase in order to operate our apparatus. We do not believe that we altered the composition of the wax enough to have significantly altered its properties.